

Misc-GAN: A Multi-Scale Generative Model for Graphs

Dawei Zhou^{†,*}, Lecheng Zheng[†], Jiejun Xu[‡], and Jingrui He[†]

[†]Arizona State University, [‡]HRL Laboratories, LLC.

Correspondence*:

Jingrui He, jingrui.he@asu.edu

2 ABSTRACT

3 Characterizing and modeling the distribution of a particular family of graphs are essential for
4 studying real-world networks in a broad spectrum of disciplines, ranging from market-basket
5 analysis to biology, from social science to neuroscience. However, it is unclear how to model
6 the complex graph organizations and learn generative models from an observed graph. The
7 key challenges come from the non-unique, high-dimensional nature of graphs, as well as the
8 graph community structures at different granularity levels. In this paper, we propose a multi-scale
9 graph generative model named *Misc-GAN*, which models the underlying distribution of the graph
10 structures at different levels of granularity, and then ‘transfers’ such hierarchical distribution from
11 the graphs in the domain of interest to a unique graph representation. The empirical results on
12 both synthetic and real data sets demonstrate the effectiveness of the proposed framework.

1 INTRODUCTION

13 Graph is a fundamental tool for depicting and modeling complex systems in various domains, ranging from
14 market-basket analysis to biology, from social science to neuroscience. Characterizing and modeling the
15 distribution of a particular family of graphs are essential in many real-world applications. For example, in
16 financial fraud detection, generative models are adopted to produce synthetic financial networks, when the
17 empirical studies need to be conducted by the third parties without divulging the private information Fich
18 and Shivdasani (2007); in drug discovery and development, sampling from the generic model can facilitate
19 the discovery of new medicines which equip with new configurations while preserving the property of the
20 existing medicines Gómez-Bombarelli et al. (2016); in social network analysis, the distributions on graphs
21 can be used to discover new graph structures and generate the evolving graphs You et al. (2018a).

22 Generative models of graphs have been well studied for decades. Traditional graph generative
23 models Erdős and Rényi (1959); Albert and Barabási (2002); Leskovec et al. (2010) are usually built
24 upon some structural premises, e.g., heavy tails for the nodes’ degree distribution, small diameters, and
25 densification in graph evolution. More recent studies on the deep generative models, e.g., Goodfellow et al.
26 (2014); Kingma and Welling (2013), reveal a surge of research interest in modeling graphs. For example,
27 Liu et al. (2017) proposes a deep model for learning characteristic topological features from the given
28 graphs via generative adversarial networks (GAN); You et al. (2018a) uses a deep autoregressive model to
29 efficiently learn the complex joint probability of all the nodes and edges from an observed set of graphs.

*Dawei Zhou and Lecheng Zheng contributed equally to this work.

30 However, real-world networks typically exhibit hierarchical distribution over graph communities, while
31 the existing graph generative models are either restricted to certain structural premises Erdős and Rényi
32 (1959); Albert and Barabási (2002); Leskovec et al. (2010) or unable to capture the hierarchical community
33 structures over the graphs Grover et al. (2018); Li et al. (2018); Simonovsky and Komodakis (2018).
34 Developing graph generative models that can capture not only the low connectivity patterns at the level of
35 individual nodes and edges, but also the higher-order connectivity patterns, i.e., the hierarchical community
36 structures in the given graphs, will significantly improve the fidelity of graph generative models and help
37 reveal more intriguing patterns in various domains. For instance, given an author-collaborative network,
38 research groups of well-established and closely collaborated researchers could be identified by the existing
39 graph clustering methods in the lower-level granularity. While, from a coarser level, we may find these
40 research groups constitute large-scale communities which correspond to various research topics or subjects.
41 Moreover, different from image data or text data, a graph with n nodes can be represented by $n!$ equivalent
42 adjacency matrices with node permutation, which increases the difficulty of training the generative model
43 in the first place.

44 In this paper, we aim to address the following two open questions: (*Q1*) How to capture the community
45 structures at different levels of granularity and generate a unique graph representation that preserves such
46 hierarchical graph structures? (*Q2*) How to alleviate the high complexity of modeling the numerous
47 representations of graphs and ensure the fidelity of the proposed graph generative model? To address
48 the preceding challenges, we propose a generic generative model of graphs (*Misc-GAN*) to learn the
49 underlying distribution of graph structures at different levels of granularity. In particular, our proposed
50 framework consists of three key steps. First, it coarsens the input graph into the structured representations
51 of different levels (i.e., granularity). Then, inspired by the success of deep generative models in image
52 translation Goodfellow et al. (2014); Kingma and Welling (2013), a cycle-consistent adversarial network
53 (CycleGAN) Zhu et al. (2017) is adopted to learn the graph structure distribution and generate a synthetic
54 coarse graph at each granularity level. At last, the *Misc-GAN* framework defines a reconstruction process,
55 which reconstructs the graphs at each granularity level and aggregates them into a unique representation.

56 The main contributions of this paper can be summarized from three aspects:

- 57 1. A novel problem setting which aims to model the complex distribution of community structures at
58 different granularity levels in the real networks.
- 59 2. A graph generative model which is capable of modeling hierarchical topology features from single or a
60 set of observed graphs and produce high-quality domain specific synthetic graphs.
- 61 3. Extensive experiments and case-studies on both real and synthetic data sets, showing the effectiveness of
62 the proposed framework *Misc-GAN*.

63 The rest of this paper is organized as follows. We briefly review some related work in Section 2,
64 formally define the multi-scale domain adaptive graph generation problem in Section 3 and present the
65 formulation and implementation of our proposed *Misc-GAN* framework in Section 4. The empirical studies
66 are conducted in Section 5. Finally, we conclude this paper in Section 6.

2 RELATED WORK

67 In this section, we briefly review the related studies on the generative adversarial network, multi-scale
68 analysis of graph and cycle consistency.

69 2.1 Generative Adversarial Network

70 In Goodfellow et al. (2014), the authors propose the generative adversarial networks (GANs) to create a
 71 generative model and a discriminative model and compete them with each other in the adversarial setting.
 72 The authors denote $P_z(z)$ to be the prior of the input noise variables z and $G(z; \theta_g)$ to represent a mapping
 73 to data space, where G is a differentiable function represented by a multi-layer perceptron with parameters
 74 θ_g . $G(z)$ maps the noise variables to data space and it aims to generate samples as genuine as possible. The
 75 authors also define $D(x; \theta_d)$ to be another multi-layer perceptron or discriminator distinguishing whether
 76 the given samples are drawn from the real-world data set or from the fake data set. $D(x)$ is the probability
 77 of x coming from the real-world data set rather than the generated data set. In this min-max game, the
 78 discriminator D aims to maximize the probability of assigning the correct label to both the real samples and
 79 the faked samples generated by the generator G , while the generator G aims to minimize the probability
 80 that the discriminator D successfully distinguishes the faked samples from the real samples. The objective
 81 of this min-max game is written as:

$$\min_G \max_D V(G, D) = \mathbb{E}_{x \sim P_{data}(x)} [\log D(x)] + \mathbb{E}_{z \sim P_z(z)} [\log(1 - D(G(z)))] \quad (1)$$

82 In this paper, generative adversarial network is the basis to transfer graphs from one domain to another
 83 domain, and meanwhile, the local valuable structures of graphs are preserved.

84 2.2 Multi-Scale Analysis of Graphs

85 Multi-scale analysis of graphs has been studied for years in machine learning with wide applications in
 86 numerous areas, such as simplification and compression of graphs Safro and Temkin (2011); Cour et al.
 87 (2005), dynamics of graphs at different resolutions Lee and Maggioni (2011); Gao et al. (2016), graph
 88 visualization Stolte et al. (2003), recommendation systems Gou et al. (2011) and so on. The common
 89 assumption of multi-scale analysis is that the given data in a high dimensional space has a much lower
 90 dimensional intrinsic geometry. Take the document text as an example, the dependencies among words
 91 constrain the distribution of word frequency in a lower dimensional space. Diffusion wavelets Coifman
 92 and Maggioni (2006) is one common method used in multi-scale analysis which allows us to construct
 93 functions on the graph for statistical learning tasks by producing coarser and coarser graphs at different
 94 resolution levels. In this paper, we adopt the concept of multi-scale analysis to capture the local structure of
 95 graphs at different resolution levels and then reconstruct the graph while preserving these important local
 96 structures.

97 2.3 Cycle Consistency

98 The concept of cycle consistency has been applied to various computer vision problems, including image
 99 matching Huang and Guibas (2013); Zhou et al. (2015), co-segmentation Wang et al. (2013, 2014), style
 100 transfer Zhu et al. (2017); Chang et al. (2018), and structure from motion Zach et al. (2010); Wilson and
 101 Snavely (2013). The idea of cycle consistency constrain is utilized as a regularizer in these algorithms,
 102 such as cycle consistency loss used in Zhou et al. (2016); Godard et al. (2017) to push the mappings to be
 103 as consistent with each other as possible in the supervised convolution neural network training. Zhu et al.
 104 (2017) proposes the Cycle-Consistent generative adversarial network to learn two mappings or generators
 105 $G : X \rightarrow Y$ and $F : Y \rightarrow X$ between two domains X and Y . The authors introduce two adversarial
 106 discriminators D_X and D_Y , where D_X aims to distinguish the images x drawn from the real data set X
 107 from the fake images generated by $F(Y)$; similarly, D_Y aims to distinguish the images y drawn from data

108 set Y from the fake images generated by $G(X)$. In this paper, we apply this concept to find the graph
 109 transfer mappings between domain X and domain Y , such that the transferred graph from domain Y to
 110 domain X is sufficiently similar to the graph in domain X .

3 PROBLEM DEFINITION

111 In this section, we introduce the notation and problem definition of this paper. The main symbols and
 112 notations are summarized in Table 1. We use ordinary lowercase letters to denote scalars, boldface lowercase
 113 letters to denote vectors, and boldface uppercase letters to denote matrices and tensors. Moreover, the
 114 elements (e.g., entries, fibers and slices) in a matrix or a tensor are represented in the same way as the
 115 Matlab, e.g., $M(i, j)$ is the element at the i^{th} row and j^{th} column of the matrix M , and $M(i, :)$ is the i^{th}
 116 row of M , etc.

Table 1. Symbols and Notations.

Symbol	Definition and Description
G_s, G_t	the source domain graph and the target domain graph
\tilde{G}_t	the generated graph of the target domain
$\mathbf{A}_s, \mathbf{A}_t, \tilde{\mathbf{A}}_t$	the adjacency matrices of G_s, G_t and \tilde{G}_t
V_s, V_t	the sets of nodes in G_s and G_t
E_s, E_t	the sets of edges in G_s and G_t
$G_s^{(l)}, G_t^{(l)}$	the induced l -th granularity coarse graphs of G_s and G_t
n_s, n_t	number of nodes in G_s and G_t
m_s, m_t	number of edges in G_s and G_t
L	number of granularity levels
$\mathcal{F}^{(l)}, \mathcal{B}^{(l)}$	the generators in the forward and backward GAN at the l -th layer
$D_{\mathcal{F}}^{(l)}, D_{\mathcal{B}}^{(l)}$	the discriminators in the forward and backward GAN at the l -th layer

117 The goal of this paper is to generate a synthetic target domain graph \tilde{G}_t , by learning mapping functions
 118 between the source domain graph G_s and the target domain graph G_t . Without loss of generality, in this
 119 paper, we assume that there exists a universal structure distribution p_{data} , which defines the structural role
 120 of each entity, i.e., node, edge, and subgraph, of the observed graphs. Many existing graph generative
 121 models Bojchevski et al. (2018); You et al. (2018b) are designed to learn the structure distribution of G at a
 122 single scale, and therefore they might overlook some intriguing patterns in the underlying networks, e.g.,
 123 the multi-level cluster-within-cluster structures Ravasz and Barabási (2003). Fig. 1 presents an illustrative
 124 example of the hierarchical structures in collaboration networks. In particular, the graph exhibits four-level
 125 hierarchies including (L1) all the entities in the collaboration network, (L2) early-stage researchers, (L3)
 126 mid-career researchers and (L4) senior researchers. It is unclear how to characterize such hierarchical
 127 structures and generate domain-specific synthetic graphs. Moreover, the generative model needs to be
 128 scalable when modeling large-scale networks that have exponentially many representations. With the above
 129 notations and objects, we formally define our problem as follows:

130 **PROBLEM 1. Multi-Level Structure-Preserving Graph Generation**

131 **Input:** (i) a target domain graph $G_t = (V_t, E_t)$, (ii) a source domain graph $G_s = (V_s, E_s)$, (iii) the number

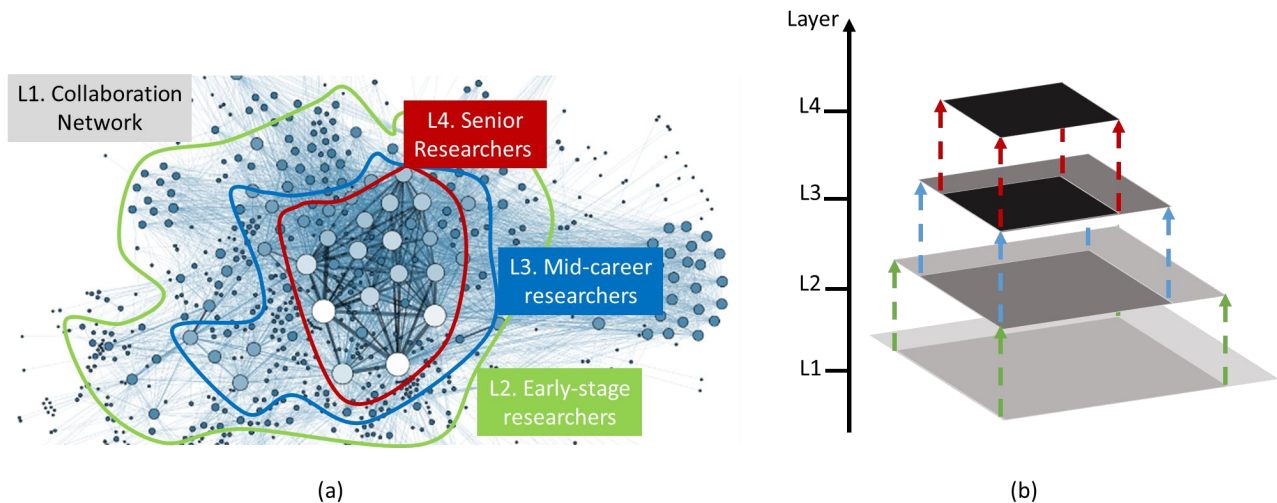


Figure 1. An illustration example. (a) presents a visualization of the collaboration network Grandjean (2016). (b) shows the hierarchical structure of the research communities, from early-stage researchers to mid-career researchers and senior researchers.

132 of granularity levels L .

133 **Output:** (i) a mapping function \mathcal{F} that can translate any source-domain graphs to the corresponding target
 134 domain graphs while preserving the hierarchical structure distribution over the observed target graph G_t ,
 135 (ii) a generated synthetic target domain graph \tilde{G}_t .

4 PROPOSED FRAMEWORK

136 In this section, we present our multi-scale graph generative model *Misc-GAN*, which simultaneously
 137 characterize and model the structural distribution of the observed graphs at multiple scales. In particular,
 138 we first formulate our framework into a generic optimization problem, and then discuss the details on three
 139 modules, i.e., multi-scale graph representation module, graph generation module, and graph reconstruction
 140 module, in our proposed framework 2.

141 4.1 A Generic Joint Learning Framework

142 To address the proposed problem of multi-level structure-preserving graph generation, our joint learning
 143 framework should primarily focus on the following aspects. First (*problem setting*), the existing methods
 144 are mainly restricted to a single granularity level of graph structures, which might increase the possibility
 145 of overlooking the hierarchical community structures in the observed graphs. Thus, the graph generation
 146 model should be able to capture the community structures at multiple levels of granularity and generate a
 147 unique graph representation. Second (*graph generation performance*), it is unclear how to alleviate the
 148 high complexity and ensure the fidelity of the graph generation. This is crucial especially if the observed
 149 graphs are noisy and large-scale. With these objectives in mind, we propose a generic graph generation
 150 framework as an optimization problem with the following objective function:

$$\begin{aligned}
\mathcal{L} &= \mathcal{L}_{ms} + \mathcal{L}_{\mathcal{F}} + \mathcal{L}_{\mathcal{B}} + \mathcal{L}_{cyc} \\
&= KL\left(\underbrace{\sum_{l=1}^L w^{(l)} \mathcal{F}^{(l)}(G_s^{(l)}) + b, G_t}_{\mathcal{L}_{ms}: \text{multi-scale reconstruction loss}}\right) \\
&\quad + \underbrace{\alpha \sum_{l=1}^L \mathbb{E}_{G_t^{(l)} \sim P_{data}(G_t^{(l)})} [\log D_{\mathcal{F}}^{(l)}(G_t^{(l)})] + \mathbb{E}_{G_s^{(l)} \sim P_{data}(G_s^{(l)})} [\log(1 - D_{\mathcal{F}}^{(l)}(\mathcal{F}(G_s^{(l)})))]}_{\mathcal{L}_{\mathcal{F}}: \text{forward adversarial loss}} \\
&\quad + \underbrace{\beta \sum_{l=1}^L \mathbb{E}_{G_s^{(l)} \sim P_{data}(G_s^{(l)})} [\log D_{\mathcal{B}}^{(l)}(G_s^{(l)})] + \mathbb{E}_{G_t^{(l)} \sim P_{data}(G_t^{(l)})} [\log(1 - D_{\mathcal{B}}^{(l)}(\mathcal{B}^{(l)}(G_t^{(l)})))]}_{\mathcal{L}_{\mathcal{B}}: \text{backward adversarial loss}} \\
&\quad + \underbrace{\gamma \sum_{l=1}^L \mathbb{E}_{G_s^{(l)} \sim P_{data}(G_s^{(l)})} [\|\mathcal{B}^{(l)}(\mathcal{F}^{(l)}(G_s^{(l)})) - G_s^{(l)}\|_1] + \mathbb{E}_{G_t^{(l)} \sim P_{data}(G_t^{(l)})} [\|\mathcal{F}^{(l)}(\mathcal{B}^{(l)}(G_t^{(l)})) - G_t^{(l)}\|_1]}_{\mathcal{L}_{cyc}: \text{cycle consistency loss}}
\end{aligned}$$

151 where the objective consists of four terms. The first term L_{ms} is the multi-scale reconstruction loss, which
152 is designed to minimize the Kullback-Leibler (KL) divergence Moreno et al. (2004) between the target
153 graph G_t and the generated graph \tilde{G}_t , i.e., $\tilde{G}_t = \sum_{l=1}^L w^{(l)} \mathcal{F}(G_s^{(l)}) + b$. We generalize the conventional
154 KL divergence to our problem setting to compare two graphs as follows

$$KL(\tilde{G}_t, G_t) = \sum_{i=1}^n \sum_{j=1}^n (A_t(i, j) + \epsilon) \log \frac{A_t(i, j) + \epsilon}{\tilde{A}_t(i, j) + \epsilon} \quad (2)$$

155 where A_t and \tilde{A}_t are the adjacency metrics of \tilde{G}_t and G_t , ϵ is a constant with a small value to avoid $\log(0)$
156 or division by 0. The second term $\mathcal{L}_{\mathcal{F}}$ learns a forward mapping function \mathcal{F} from the source graph G_s to G_t .
157 The discriminator $D_{\mathcal{F}}^{(l)}$ aims to figure out whether the given graph is a real graph from the target domain or
158 a fake graph generated by the generator \mathcal{F} which is transferred from the source domain graph. Similar to
159 the second term, the third term $\mathcal{L}_{\mathcal{B}}$ defines a backward adversarial loss, which aims to learn the mapping
160 function from the target domain to the source domain. The fourth term \mathcal{L}_{cyc} is the cycle consistency loss,
161 which is introduced to further reduce the space of possible mapping function. We argue that learning such
162 bi-directional mapping can largely prevent the learned mapping functions from contradicting each other.
163 At last, we also introduce three positive constants, i.e., α, β, γ , to balance the impact of these four terms in
164 the overall objective function. Follow the min-max scheme of GAN, we aim to solve:

$$\mathcal{F}^{*(l)}, w^{*(l)}, b^* = \arg \min_{\mathcal{F}^{(l)}, \mathcal{B}^{(l)}, w^{(l)}, b} \max_{D_{\mathcal{F}}^{(l)}, D_{\mathcal{B}}^{(l)}} \mathcal{L}, l = 1, \dots, L \quad (3)$$

165 **4.2 Network Architecture**

166 Here, we present our *Misc-GAN* framework (Fig. 2). Overall, our framework can be separated into
 167 three stages (i.e., modules). In the first stage, our framework takes the input graphs G_t and explores
 168 the hierarchical structures by constructing the coarse graphs in L levels of granularity (w.r.t. L layers in
 169 Fig. 2). In the second stage, our framework trains an independent graph generative model and produces
 170 the multi-scale coarse graph in each layer. In the third stage, our framework autonomously combines the
 171 outputs from the previous stage to construct the synthetic graph \tilde{G}_t that preserves the hierarchical topology
 172 features of the given graphs G_t .

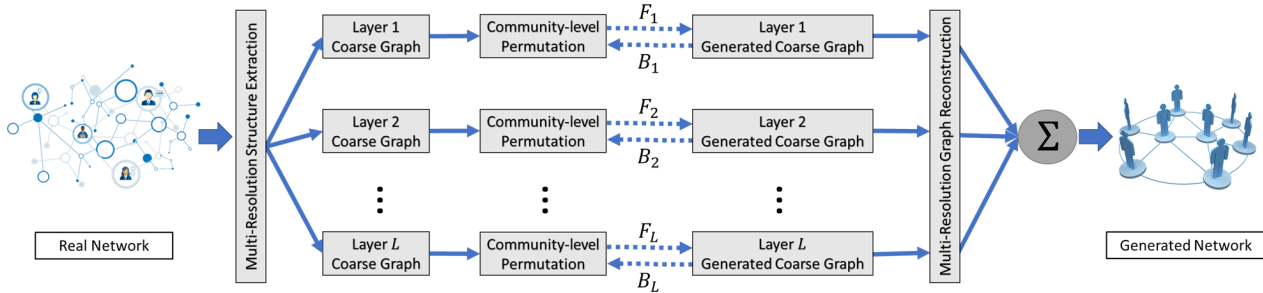


Figure 2. The proposed *Misc-GAN* framework.

173 **Multi-Scale Graph Representation Module.** In this module, we explore the hierarchical cluster-within-
 174 cluster structures in order to better characterize the given graph G_t , by using the multi-scale approaches,
 175 e.g., hierarchical clustering Johnson (1967), algebraic multigrid (AMG) Ruge and Stüben (1987). In
 176 particular, given a symmetric matrix A_t , the multi-scale approaches recursively construct a multi-scale
 177 hierarchy of increasingly coarser graphs as follows

$$P^{(l-1)'} \dots P^{(1)'} A_t P^{(1)} \dots P^{(l-1)} = A_t^{(l)} \quad (4)$$

178 where $l = 1, \dots, L$, $P^{(1)}, \dots, P^{(l-1)}$ are the coarsening operators, and A_l is the coarse graph at the l -th
 179 layer. Based on Eq. 4, we construct a set of coarse graphs with multiple scales from the target domain
 180 graph G_t . These coarse graphs will be fed into the following graph generative module in order to learn the
 181 hierarchical structures of G_t .

182 **Graph Generation Module.** It is challenging to learn the underlying structure distribution p_{data} of the
 183 target domain graph G_t , as the graph with n nodes can be represented by $n!$ equivalent adjacency matrices
 184 with node permutations You et al. (2018a). Some recent works have been proposed to tackle this issue.
 185 For example, Simonovsky and Komodakis (2018) proposes an approximate graph matching scheme that
 186 requires $O(n^4)$ operations in the worst case; You et al. (2018a) develops a tree-structure node ordering
 187 scheme, which is based on breadth-first-search (BFS) to reduce the computational complexity. However,
 188 these methods may either suffer from the intractable time complexity, or not well preserve the hierarchical
 189 structures of the given networks.

190 Here, we propose a multi-scale graph generation scheme, which models the complex distribution of graph
 191 structures over a pyramid of coarse graphs rather than the original graphs. The intuitions are in the following
 192 two aspects: (1) directly training from the coarse graphs facilitates the learning process of the generative
 193 model, as the coarse graphs serve as the abstractions of the original graphs; (2) this scheme provides the
 194 flexibility for the users to decide the granularity-level of the coarse graphs to be learned, which could be
 195 attractive when we need to model the large-scale networks. To be more specific, the graph generation

196 module at each layer (shown in Fig. 2) can be separated into three steps: First, we partition the graph into
 197 multiple non-overlapping subgraphs using state-of-the-art graph clustering methods Ester et al. (1996);
 198 Schaeffer (2007). Then, based on the detected communities, we generate a set of block diagonal matrices by
 199 shuffling community blocks over the diagonals, which are used to characterize the community-level graph
 200 structures. At last, the generated block diagonal matrices are fed into an independent graph generative
 201 model to generate the synthetic coarse graphs at each layer.

202 **Graph Reconstruction Module.** In this stage, we first adopt the multi-scale approaches to reconstruct
 203 the graph from coarse to fine as follows

$$\mathbf{R}^{(1)'} \dots \mathbf{R}^{(l-1)'} \mathbf{A}_t^{(l)} \mathbf{R}^{(l-1)} \dots \mathbf{R}_1 = \tilde{\mathbf{A}}_t^{(l)} \quad (5)$$

204 where $l = 1, \dots, L$, $\mathbf{R}^{(1)}, \dots, \mathbf{R}^{(l-1)}$ are the reconstruction operations, and $\tilde{\mathbf{A}}_t^{(l)}$ is the reconstructed
 205 adjacency matrix from the l -th layer. After that, all the reconstructed graphs are in the same scale as the
 206 target graph G_t , which could be aggregated into a unique one by a linear function, $\tilde{\mathbf{A}}_t = \sum_{l=1}^L w^{(l)} \tilde{\mathbf{A}}_t^{(l)} + b$,
 207 where $w^{(1)}, \dots, w^{(L)}$ are the non-negative weights, and b is a bias.

208 4.3 Training Details

209 We apply the technique of cycleGAN to transfer graph from one domain to another domain. Different
 210 from the density property of images, the adjacency matrix for a graph is much sparser. In our algorithm,
 211 two convolution layers are used to capture the hierarchical structure information of the graph. Because
 212 the adjacency matrix of a graph is sparser than the dense matrix of an image, we set the size of stride to
 213 be 4, the size of kernels to be 4×4 matrices, and the number of kernels to be 32 for each convolution
 214 layer. Then, k iterations of ResNet He et al. (2016) are applied to accelerate the convergence. Finally, two
 215 deconvolution layers are used to reconstruct the adjacency matrix with similar settings used in convolution
 216 layers.

217 Second, following the strategy mentioned in Shrivastava et al. (2017); Zhu et al. (2017), we update two
 218 discriminators with the history of the generated graph $\tilde{\mathbf{A}}_t^{(l)}$ in the l -th layer to reduce the vibration of the
 219 model. For all the experiments, we set the training iterations to be 250. Adam solver Kingma and Ba (2014)
 220 with a batch size of 1 is used to minimize the loss function, and all networks are trained with a learning
 221 rate of 0.0002 in the tensorflow deep learning framework.

5 EXPERIMENT

222 In this section, we demonstrate the performance of our proposed *Misc-GAN* framework on real networks.
 223 Moreover, we present a case study to illustrate the effectiveness of *Misc-GAN* in learning the topological
 224 features at different levels of granularity.

225 5.1 Experiment Setup

226 **Data sets:** We evaluate our proposed algorithm on seven real-world networks from the Stanford Network
 227 Analysis Project (SNAP) Leskovec and Krevl (2015). The statistics of data sets are summarized in Table 2.
 228 In particular, Email is a communication network, where an edge exists if one person sends at least one email
 229 to another person; Facebook is a social network, where each edge represents a social connection between
 230 the users in Facebook; Wiki is a voting network, which is used by Wikipedia to elect administrators among
 231 the huge contributors; P2P is a file-sharing network, where each node represents a host and each edge

Network	Type	Nodes	Edges
Email	Directed	1,005	25,571
Facebook	Undirected	4,039	88,234
Wiki	Directed	8,292	14,547,910
P2P	Directed	10,876	39,994
Gnu	Directed	6,301	20,777
Bitcoin	Directed	5,881	35,592
CA	Undirected	5,242	14,496

Table 2. Statistics of the network data sets.

232 represents a connection between hosts; GNU is another Gnutella peer-to-peer file sharing network, which is
 233 similar to P2P network; Bitcoin is a who-trusts-whom network that covers the bitcoin trading information
 234 on the Bitcoin OTC platform, where each node represents a user and each edge represents the trustfulness
 235 between two users; CA is a collaboration network from arXiv, where each node represents an author and
 236 each edge represents the collaborations between authors. For different weights in a graph, i.e., Bitcoin
 237 graph, we convert the values of edges to binary values in order to feed them to our model.

238 **Comparison Methods:** We compare *Misc-GAN* with two random graph models, i.e., Erdős-Rényi (E-R)
 239 model Erdős and Rényi (1959) and Barabási-Albert (B-A) model Albert and Barabási (2002), and one
 240 recent deep graph generative model, i.e., GAE Kipf and Welling (2016). All the graph statistics are outlined
 241 in Table 2. In our setting, the graphs in Table 2 are target domain graphs, and the source domain graphs
 242 are generated under a random normal distribution with the same numbers of nodes and edges as the target
 243 domain graphs.

244 **Repeatability:** All the data sets are publicly available. We will release the code of our algorithms through
 245 the authors' website after the paper is published. The experiments are performed on a Windows machine
 246 with four 3.5GHz Intel Cores and 256GB RAM.

247 5.2 Quantitative Evaluation

248 The comparison results in terms of effectiveness across a diverse set of real networks are shown in Fig. 3.
 249 In particular, we present the results regarding the following metrics: (1) AD: the average degree of all nodes
 250 in a graph; (2) LCC: the size of the largest connected component of the graph; (3) EPL: the exponent of the
 251 power law distribution of the graph; (4) GC: the Gini coefficient of the degree distribution of the graph; (5)
 252 KL: the symmetric Kullback-Leibler (KL) divergence Moreno et al. (2004) between the local clustering
 253 coefficient distributions of the original graphs and the generated graphs; (6) Graph Kernel: the similarity
 254 between the original graph and the generated one by using the random-walk based graph kernel Kang et al.
 255 (2012). From these figures, the x-axis of each figure represents a data set, and the y-axis is the value of
 256 metrics. From Fig. 3 (a) to Fig. 3 (d), we mainly compare various graph statistics between the original
 257 graph and the generated ones using baseline methods. If the value of the metric of the generated graph is
 258 close to that of the original graph, it means the generated graph is much more similar to the original graph.
 259 We observe that the AD of our proposed algorithm is almost identical to the AD of the original graph for
 260 all data sets; for the other three metrics, our proposed algorithm also outperforms the others in most cases.
 261 In Fig. 3 (e) and Fig. 3 (f), we present the divergence and similarity score between the original graphs and
 262 the generated graphs. Note that, for presentation purposes, all the results in Fig. 3 (e) and Fig. 3 (f) are
 263 presented using a negative log function, i.e., $f(x) = -\log(x)$. In general, we observe that (1) our proposed
 264 *Misc-GAN* outperforms the comparison methods across most of the datasets and evaluation metrics in most
 265 cases. For example, in the Email data, *Misc-GAN* is 66% smaller on the clustering coefficient distribution

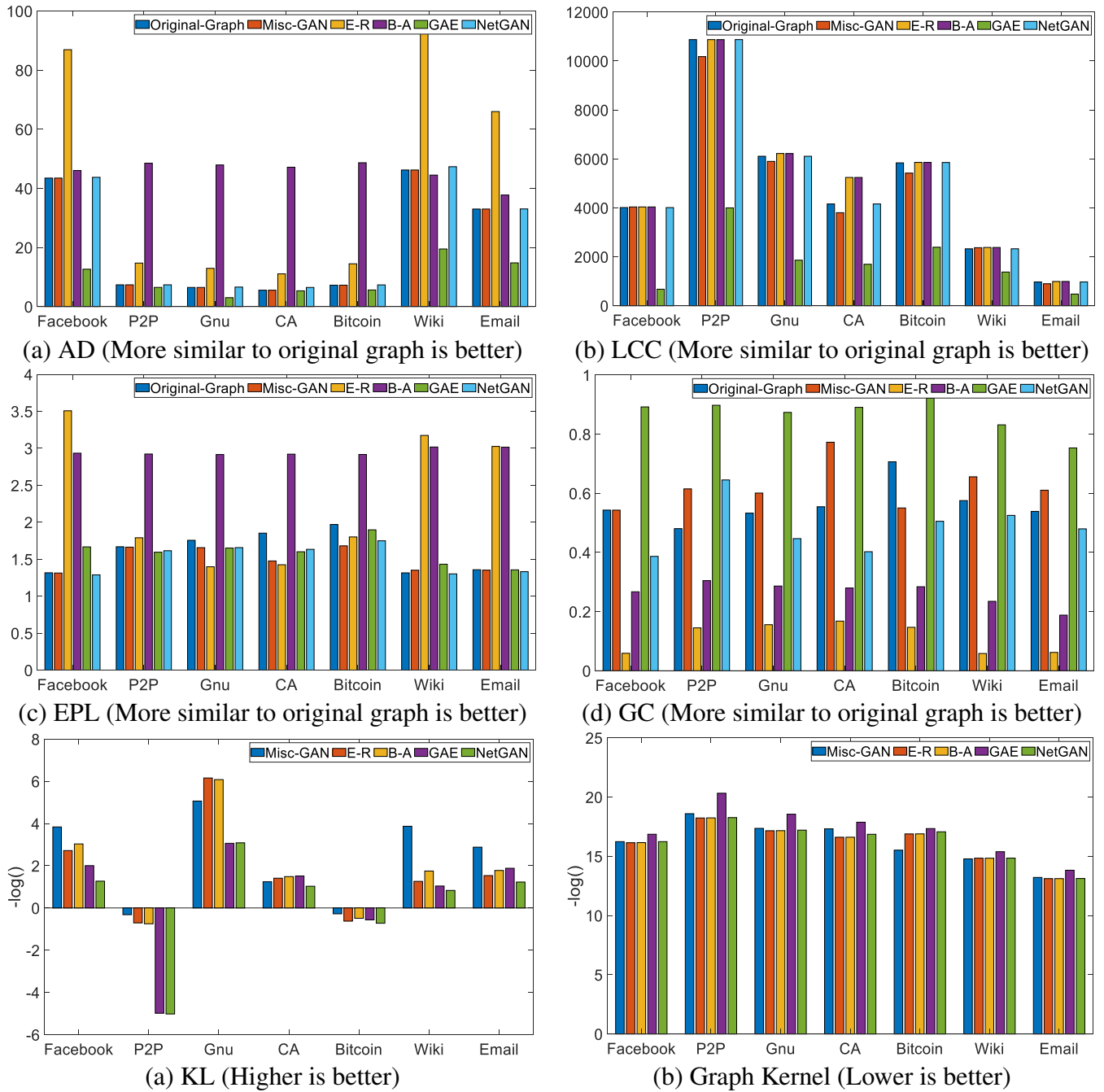


Figure 3. Effectiveness analysis.

266 evaluation; (2) our proposed *Misc-GAN* framework better preserves the local topological features (e.g., the
 267 largest connected component and local clustering coefficient) and the global features (e.g., mean degree,
 268 the power law coefficients of the degree distribution of graphs) than other deep generative models (e.g.,
 269 GAE). It is because our method explores the network structures at multiple resolutions and automatically
 270 learns the weights regarding the importance of topological features at different levels, while the existing
 271 deep generative models may fail to model such fine-grained topological features.

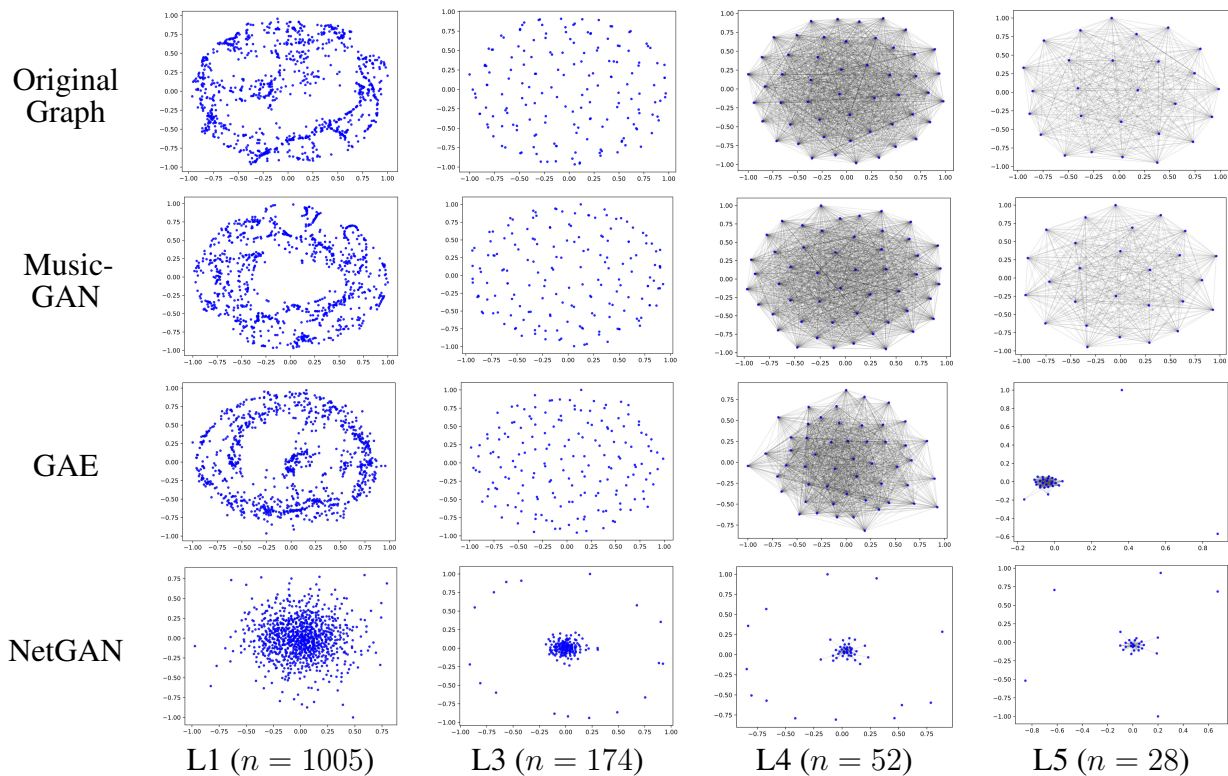


Figure 4. Graph reconstruction at multiple scales.

272 5.3 A Case Study with respect to the Impact of Multi-Scale Analysis

273 A simple but intuitive way to evaluate the generated graphs is to visualize the network layout in a
 274 two-dimensional space. In Fig. 4, we compare the multi-scale network representations of the original graph
 275 (i.e., Email) and the generated graphs. In particular, we select the deep generative model GAE and NetGAN
 276 as our baseline methods and construct coarse graphs at four different scales based on Eq. 4. In general,
 277 we find that (1) our framework well preserves the graph structures at multiple levels of granularity; (2)
 278 NetGAN only preserves the lower-level connectivity patterns (e.g., clusters within a loop pattern) in Layer
 279 1, but fails in capturing the higher-level connectivity patterns (e.g., the cluster of super-nodes) in Layer
 280 3, Layer 4 and Layer 5. The reason for the preceding phenomenon is that NetGAN is trained at a single
 281 level (i.e., a single granularity of nodes), which results in the coarse reconstruction of high-level network
 282 structures. GAE also has the similar problem due to the failure to capture the higher-level connectivity
 283 patterns(i.e., in Layer 5).

6 CONCLUSION

284 We propose a multi-scale generative model named *Misc-GAN* for graph-structured data, which explores
 285 the network structures at multiple resolutions and automatically generates a unique graph representation
 286 that preserves such fine-grained topological features. The empirical studies show that *Misc-GAN* achieves
 287 significantly better performance compared to the state-of-the-art models on real networks. However, various
 288 challenges remain in this problem, such as how to make the deep generative model scale to massive graphs,
 289 and how to generate the domain-specific graph with complex connectivity patterns (e.g., modeling the
 290 online transaction networks with money laundering patterns)?

ACKNOWLEDGMENT

291 This work is supported by the United States Air Force and DARPA under contract number FA8750-17-C-
292 0153 , National Science Foundation under Grant No. IIS-1552654, and Grant No. CNS-1629888, the U.S.
293 Department of Homeland Security under Grant Award Number 2017-ST-061-QA0001, and an IBM Faculty
294 Award. The views and conclusions are those of the authors and should not be interpreted as representing
295 the official policies of the funding agencies or the government.

REFERENCES

- 296 Albert, R. and Barabási, A. (2002). Statistical mechanics of complex networks. *Reviews of modern physics*
- 297 Bojchevski, A., Shchur, O., Zügner, D., and Günnemann, S. (2018). Netgan: Generating graphs via
298 random walks. In *Proceedings of the 35th International Conference on Machine Learning, ICML 2018,*
299 *Stockholmsmässan, Stockholm, Sweden, July 10-15, 2018.* 609–618
- 300 Chang, H., Lu, J., Yu, F., and Finkelstein, A. (2018). Pairedcyclegan: Asymmetric style transfer for
301 applying and removing makeup. In *2018 IEEE Conference on Computer Vision and Pattern Recognition*
302 *(CVPR)*
- 303 Coifman, R. R. and Maggioni, M. (2006). Diffusion wavelets. *Applied and Computational Harmonic*
304 *Analysis* 21, 53–94
- 305 Cour, T., Benezit, F., and Shi, J. (2005). Spectral segmentation with multiscale graph decomposition. In
306 *Computer Vision and Pattern Recognition, 2005. CVPR 2005. IEEE Computer Society Conference on*
307 *(IEEE)*, vol. 2, 1124–1131
- 308 Erdős, P. and Rényi, A. (1959). On random graphs, i. *Publicationes Mathematicae (Debrecen)*
- 309 Ester, M., Kriegel, H.-P., Sander, J., Xu, X., and etc. (1996). A density-based algorithm for discovering
310 clusters in large spatial databases with noise. In *KDD*
- 311 Fich, E. M. and Shivdasani, A. (2007). Financial fraud, director reputation, and shareholder wealth. *Journal*
312 *of Financial Economics*
- 313 Gao, Z.-K., Cai, Q., Yang, Y.-X., Dang, W.-D., and Zhang, S.-S. (2016). Multiscale limited penetrable
314 horizontal visibility graph for analyzing nonlinear time series. *Scientific reports* 6, 35622
- 315 Godard, C., Mac Aodha, O., and Brostow, G. J. (2017). Unsupervised monocular depth estimation with
316 left-right consistency. In *2017 IEEE Conference on Computer Vision and Pattern Recognition, CVPR*
317 *2017, Honolulu, HI, USA, July 21-26, 2017.* 6602–6611
- 318 Gómez-Bombarelli, R., Wei, J. N., Duvenaud, D., Hernández-Lobato, J. M., Sánchez-Lengeling, B.,
319 Sheberla, D., et al. (2016). Automatic chemical design using a data-driven continuous representation of
320 molecules. *ACS Central Science*
- 321 Goodfellow, I., Pouget-Abadie, J., Mirza, M., Xu, B., Warde-Farley, D., Ozair, S., et al. (2014). Generative
322 adversarial nets. In *NIPS*
- 323 Gou, L., You, F., Guo, J., Wu, L., and Zhang, X. L. (2011). Sfviz: interest-based friends exploration and
324 recommendation in social networks. In *Proceedings of the 2011 Visual Information Communication-*
325 *International Symposium (ACM)*, 15
- 326 [Dataset] Grandjean, M. (2016). How to display complex network data with information
327 visualization. [https://www.interaction-design.org/literature/article/
328 how-to-display-complex-network-data-with-information-visualization.](https://www.interaction-design.org/literature/article/how-to-display-complex-network-data-with-information-visualization)
329 CC BY-SA 3.0
- 330 Grover, A., Zweig, A., and Ermon, S. (2018). Graphite: Iterative generative modeling of graphs. *arXiv*
331 *preprint arXiv:1803.10459*

- 332 He, K., Zhang, X., Ren, S., and Sun, J. (2016). Deep residual learning for image recognition. In *2016*
333 *IEEE Conference on Computer Vision and Pattern Recognition, CVPR 2016, Las Vegas, NV, USA, June*
334 *27-30, 2016*. 770–778
- 335 Huang, Q. and Guibas, L. J. (2013). Consistent shape maps via semidefinite programming. *Comput. Graph.*
336 *Forum* 32, 177–186
- 337 Johnson, S. C. (1967). Hierarchical clustering schemes. *Psychometrika*
- 338 Kang, U., Tong, H., and Sun, J. (2012). Fast random walk graph kernel. In *SDM*
- 339 Kingma, D. P. and Ba, J. (2014). Adam: A method for stochastic optimization. *CoRR* abs/1412.6980
- 340 Kingma, D. P. and Welling, M. (2013). Auto-encoding variational bayes. *arXiv preprint arXiv:1312.6114*
- 341 Kipf, T. N. and Welling, M. (2016). Variational graph auto-encoders. *arXiv preprint arXiv:1611.07308*
- 342 Lee, J. D. and Maggioni, M. (2011). Multiscale analysis of time series of graphs. In *International*
343 *Conference on Sampling Theory and Applications (SampTA)*
- 344 Leskovec, J., Chakrabarti, D., Kleinberg, J., Faloutsos, C., and Ghahramani, Z. (2010). Kronecker graphs:
345 An approach to modeling networks. *JMLR*
- 346 Leskovec, J. and Krevl, A. (2015). {SNAP Datasets}:{Stanford} large network dataset collection
- 347 Li, Y., Vinyals, O., Dyer, C., Pascanu, R., and Battaglia, P. (2018). Learning deep generative models of
348 graphs. *arXiv preprint arXiv:1803.03324*
- 349 Liu, W., Cooper, H., Oh, M. H., Yeung, S., Chen, P., Suzumura, T., et al. (2017). Learning graph topological
350 features via gan. *arXiv preprint arXiv:1709.03545*
- 351 Moreno, P. J., Ho, P. P., and Vasconcelos, N. (2004). A kullback-leibler divergence based kernel for svm
352 classification in multimedia applications. In *NIPS*
- 353 Ravasz, E. and Barabási, A. (2003). Hierarchical organization in complex networks. *Physical Review E*
- 354 Ruge, J. W. and Stüben, K. (1987). Algebraic multigrid. In *Multigrid methods* (SIAM)
- 355 Safro, I. and Temkin, B. (2011). Multiscale approach for the network compression-friendly ordering.
356 *Journal of Discrete Algorithms* 9, 190–202
- 357 Schaeffer, S. (2007). Graph clustering. *Computer science review*
- 358 Shrivastava, A., Pfister, T., Tuzel, O., Susskind, J., Wang, W., and Webb, R. (2017). Learning from
359 simulated and unsupervised images through adversarial training. In *2017 IEEE Conference on Computer*
360 *Vision and Pattern Recognition, CVPR 2017, Honolulu, HI, USA, July 21-26, 2017*. 2242–2251
- 361 Simonovsky, M. and Komodakis, N. (2018). Graphvae: Towards generation of small graphs using
362 variational autoencoders. *arXiv preprint arXiv:1802.03480*
- 363 Stolte, C., Tang, D., and Hanrahan, P. (2003). Multiscale visualization using data cubes. *IEEE Transactions*
364 *on Visualization and Computer Graphics* 9, 176–187
- 365 Wang, F., Huang, Q., and Guibas, L. J. (2013). Image co-segmentation via consistent functional maps.
366 In *IEEE International Conference on Computer Vision, ICCV 2013, Sydney, Australia, December 1-8,*
367 *2013*. 849–856
- 368 Wang, F., Huang, Q., Ovsjanikov, M., and Guibas, L. J. (2014). Unsupervised multi-class joint image
369 segmentation. In *2014 IEEE Conference on Computer Vision and Pattern Recognition, CVPR 2014,*
370 *Columbus, OH, USA, June 23-28, 2014*. 3142–3149
- 371 Wilson, K. and Snavely, N. (2013). Network principles for sfm: Disambiguating repeated structures with
372 local context. In *IEEE International Conference on Computer Vision, ICCV 2013, Sydney, Australia,*
373 *December 1-8, 2013*. 513–520
- 374 You, J., Ying, R., Ren, X., Hamilton, W. L., and Leskovec, J. (2018a). Graphrnn: A deep generative model
375 for graphs. *arXiv preprint arXiv:1802.08773*

- 376 You, J., Ying, R., Ren, X., Hamilton, W. L., and Leskovec, J. (2018b). Graphrnn: Generating realistic
377 graphs with deep auto-regressive models. In *Proceedings of the 35th International Conference on*
378 *Machine Learning, ICML 2018, Stockholmsmässan, Stockholm, Sweden, July 10-15, 2018*. 5694–5703
- 379 Zach, C., Klopschitz, M., and Pollefeys, M. (2010). Disambiguating visual relations using loop constraints.
380 In *The Twenty-Third IEEE Conference on Computer Vision and Pattern Recognition, CVPR 2010, San*
381 *Francisco, CA, USA, 13-18 June 2010*. 1426–1433
- 382 Zhou, T., Krähenbühl, P., Aubry, M., Huang, Q., and Efros, A. A. (2016). Learning dense correspondence
383 via 3d-guided cycle consistency. In *2016 IEEE Conference on Computer Vision and Pattern Recognition,*
384 *CVPR 2016, Las Vegas, NV, USA, June 27-30, 2016*. 117–126
- 385 Zhou, T., Lee, Y. J., Yu, S. X., and Efros, A. A. (2015). Flowweb: Joint image set alignment by
386 weaving consistent, pixel-wise correspondences. In *IEEE Conference on Computer Vision and Pattern*
387 *Recognition, CVPR 2015, Boston, MA, USA, June 7-12, 2015*. 1191–1200
- 388 Zhu, J., Park, T., Isola, P., and Efros, A. A. (2017). Unpaired image-to-image translation using cycle-
389 consistent adversarial networks. *arXiv preprint arXiv:1703.10593*